

1 **PFOA and PFOS Diffusion through LLDPE and LLDPE Coextruded with EVOH at 22°C,**
2 **35°C, and 50°C**

3 **V. Di Battista¹, R. Kerry Rowe^{2*}, D. Patch³, and K. Weber⁴**

4 **Abstract**

5 Diffusion of perfluorooctanoate (PFOA) and perfluorooctane sulfonate (PFOS) through 0.1 mm
6 and 0.75 mm LLDPE and 0.1 mm and 0.75 mm LLDPE coextruded with ethyl vinyl alcohol
7 (denoted as CoEx) at room temperature (23°C), 35°C, and 50°C is examined. These tests had
8 negligible source depletion throughout the monitoring period, indicating limited contaminant
9 partitioning and diffusion through the LLDPE. At 483 days, 23°C receptor PFOA and PFOS
10 concentrations, c_r , were $< 8 \text{ ug/L}$ ($c_r/c_o < 3.2 \times 10^{-4}$) for all tests, and at 399 days elevated
11 temperature receptor concentrations were $< 0.4 \text{ ug/L}$ ($c_r/c_o < 1.6 \times 10^{-5}$) at 35°C and $< 0.5 \text{ ug/L}$ (c_r/c_o
12 $< 2.0 \times 10^{-5}$) at 50°C for both PFOA and PFOS. LLDPE partitioning coefficient, S_{gf} was 0.9-1.4
13 (PFOA) and 2.8-5.3 (PFOS) based on sorption tests at 23°C. Based on the best estimates of
14 permeation coefficient, $P_{g\text{CoEx}}$, for CoEx was consistently lower than $P_{g\text{LLDPE}}$. For PFOA, CoEx
15 had $P_{g\text{CoEx}} < 0.26 \times 10^{-16} \text{ m}^2/\text{s}$ at 23°C, $< 11 \times 10^{-16} \text{ m}^2/\text{s}$ (35°C), and $< 10 \times 10^{-16} \text{ m}^2/\text{s}$ (50°C) while
16 LLDPE had $P_{g\text{LLDPE}} < 3.1 \times 10^{-16} \text{ m}^2/\text{s}$ (23°C), $< 13 \times 10^{-16} \text{ m}^2/\text{s}$ (35°C), and $< 19 \times 10^{-16} \text{ m}^2/\text{s}$ (50°C).
17 For PFOS, CoEx and LLDPE had $P_{g\text{CoEx}} < 0.55 \times 10^{-16} \text{ m}^2/\text{s}$ and $P_{g\text{LLDPE}} < 3.2 \times 10^{-16} \text{ m}^2/\text{s}$ (23°C),
18 $P_{g\text{CoEx}} < 8.3 \times 10^{-16} \text{ m}^2/\text{s}$ and $P_{g\text{LLDPE}} < 40 \times 10^{-16} \text{ m}^2/\text{s}$ (35°C), and $P_{g\text{CoEx}} < 8.2 \times 10^{-16} \text{ m}^2/\text{s}$ and $P_{g\text{LLDPE}}$
19 $< 52 \times 10^{-16} \text{ m}^2/\text{s}$ (50°C). These values are preliminary and may decrease as more data comes
20 available over time. The P_g values deduced for PFOA and PFOS are remarkably lower than those
21 reported for other contaminants of concern, excepting BPA, which exhibits similar behaviour.

22 **Keywords:** PFAS, PFOA, PFOS, geomembranes, diffusion, EVOH, LLDPE, polyethylene

23 PhD student, GeoEngineering Centre at Queen's – RMC, Queen's University, Kingston,
24 Canada, K7L 3N6; E: v.di.battista@queensu.ca

- 25 ² Barrington Batchelor Distinguished University Professor and Canada Research Chair in
26 Geotechnical and Geoenvironmental Engineering, GeoEngineering Centre at Queen's – RMC,
27 Queen's University, Kingston, Canada, K7L 3N6, E: kerry.rowe@queensu.ca
- 28 ³ PhD Student, Environmental Sciences Group, Department of Chemistry and Chemical
29 Engineering, Royal Military College of Canada, Kingston, ON, Canada K7K 7B4,
30 David.Patch@rmc.ca
- 31 ⁴ Director and Associate Professor, Environmental Sciences Group, Department of Chemistry
32 and Chemical Engineering, Royal Military College of Canada, Kingston, ON, Canada K7K
33 7B4, Kela.Weber@rmc.ca
- 34 * Corresponding author

35 **1. Introduction**

36 Per- and polyfluoroalkyl substances (PFAS) are organofluoride alkyl molecules, typically 4-16
37 carbon atoms in length, with multiple fluorine atoms attached to the carbon chain. The C-F bond,
38 which is extremely stable, gives these compounds desirable properties such as chemical and
39 thermal stability (Buck et al. 2011). These substances have surfactant properties due to their
40 hydrophilic functional end groups and hydrophobic fluorinated tail (3M Company 1999a). Many
41 consumer products contain PFAS as the stability of the molecules provide desirable properties
42 allowing the chemicals to be used as protective coatings to textiles, papers, and packaging and to
43 enhance the performance of various consumer products (3M Company 1999b). There are over
44 4,000 chemicals classified as PFAS, but the most widely studied PFAS compounds,
45 perfluorooctanoate, $C_7F_{15}COOH$ (PFOA) and perfluorooctane sulfonate, $C_8F_{17}SO_3H$ (PFOS) are
46 known to be persistent environmental contaminants due to the bioaccumulative, potentially
47 carcinogenic, toxic properties of these compounds, and the chemical and thermal stability of the
48 C-F bonds, (Gallen et al. 2017; Health Canada 2018a; b; National Institute of Health Sciences
49 2020).The major manufacturers of PFOA and PFOS have ceased production of these compounds
50 in favour of alternative compounds (3M Company 2000; Buck et al. 2011).

51 Historically, PFOA has been primarily used in manufacturing of fluoropolymers, including
52 polytetrafluoroethylene. PFOS and other perfluorooctanesulfonyl fluoride based chemicals were
53 used in surface treatments of textiles (e.g., carpets, upholstery, apparel, leather), paper and
54 packaging protectors (e.g., grease repellent paper for food), and performance chemicals (e.g.,
55 coatings and coating additives, insecticides, etc.) (3M Company 1999b; Buck et al. 2011; Martin
56 et al. 2010). PFOS was a main component of aqueous film forming foam (AFFF) before production
57 of PFOS was discontinued in North America. AFFF was primarily used for suppressing

58 hydrocarbon fuel fires and fire combat training activities (Milley et al. 2018). Fire suppression and
59 training activities at locations where large amounts of fuel are stored, such as airports, have
60 resulted in PFAS contamination of the surrounding soil; a common remediation strategy for PFAS
61 contaminated soil is excavation and placement in a landfill or monofill for contaminant
62 containment (Hale et al. 2017).

63 Landfills are the ultimate destination for many consumer products, including those containing
64 PFAS, and degradation of waste and water percolation through the landfill results in leachate
65 containing PFAS, including PFOA and PFOS (Busch et al. 2010; Eggen et al. 2010; Fuertes et al.
66 2017; Gallen et al. 2017; Yan et al. 2015). Although manufacturing of PFOA and PFOS has been
67 phased out, disposal of products containing these chemicals and contaminated soil remain a source
68 of potential indirect release to the environment from landfills (Government of Canada 2012). As
69 leachate collects on the base of the landfill, the chemicals can migrate through the landfill liner,
70 via advective and diffusive processes, and contaminate the surrounding environment (Rowe 2015;
71 Rowe et al. 2004). Specific chemical composition of landfill leachates is largely dependent on the
72 waste source, composition of the landfill, and the age of the landfill (Rowe et al. 2004).

73 These chemicals are present in landfill leachates worldwide due to the ubiquity of PFOA and
74 PFOS in consumer products. A study of six untreated German landfill leachates found that PFOA
75 and PFOS accounted for 12% and 2.7% of the total PFAS in the leachates; the mean total PFAS
76 concentration of the leachates was 6086 ng/L (Busch et al. 2010). Untreated municipal solid waste
77 landfill leachate samples from four sites in northern Spain contained PFOA with concentrations
78 ranging from 387-512 ng/L and accounted for an average of 42.6% of the total mass fraction of
79 PFAS; PFOS concentrations in the landfill leachate ranged from below limit of detection to 43.5
80 ng/L (Fuertes et al. 2017). Eggen et al. (2010) sampled two landfills with clay liners and found

81 that PFOS and PFOA accounted for 20-47% and 12-24% of total PFAS in the untreated landfill
82 leachate, respectively; total PFAS concentrations were 2,191-6,123 ng/L in the leachate. Another
83 study found that leachate sampled from a MSW landfill between February 2010 and June 2010
84 had variable levels of the specific PFAS species with PFOA and PFOS concentrations ranges of
85 300-1,500 ng/L and 220-4,400 ng/L, respectively, for untreated leachate that has not been
86 recirculated in the landfill (Benskin et al. 2012). A study of 27 Australian landfills of various ages
87 and stages of closure found PFOA and PFOS present in all 27 landfills, with mean concentrations
88 of 690 ng/L and 310 ng/L, respectively, and maximum PFOA and PFOS concentrations as 7,500
89 ng/L and 2,700 ng/L, respectively (Gallen et al. 2017). Sampling of five untreated landfill leachates
90 in China found total PFAS concentrations ranging from 7,280-292,000 ng/L, with PFOA
91 accounting for a mean of 36.8% (Yan et al. 2015).

92 The presence of these contaminants in landfills of various ages and locations highlights the need
93 to understand the factors affecting their transport through the landfill liner components. The ability
94 of the landfill to contain these contaminants depends on the existing liner system. Common
95 materials used as liners are geomembranes, sheets of polyethylene 1.0-2.0 mm thick.
96 Geomembranes are used worldwide for contaminant containment in landfills, and provide an
97 advective barrier for contaminant migration such that molecular diffusion is the dominant
98 contaminant transport mechanism (Rowe et al. 2004).

99 Multiple factors impact a geomembrane's diffusive characteristics. These factors are influenced
100 by properties of the contaminant and geomembranes. One critical factor is the similarity (i.e.,
101 polarity and hydrophobicity) of the contaminant to the geomembrane, such that contaminant
102 species will impact the diffusivity through a polyethylene geomembrane. In general, acids will
103 have lower permeation coefficients than nitroderivatives, aldehydes, ketones, esters, ethers, and

104 aromatic and chlorinated hydrocarbons. Benzene, toluene, ethylbenzene, xylenes (BTEX), and
105 trichloroethylene can easily diffuse through polyethylene geomembranes due to the similarity in
106 polarity of the polyethylene and the contaminants (August and Tatzky 1984; Park et al. 1995; Park
107 and Nibras 1993; Rowe et al. 2004; Sangam and Rowe 2001, 2005). Organic contaminants with
108 greater *n*-octanol/water coefficients ($\log K_{ow}$), a measure of hydrophobicity, and molecular
109 weights (M_w) are more likely to partition to polyethylene, and greater molecular weights will
110 reduce the diffusion coefficients (Park and Nibras 1993; Rowe et al. 2004; Sangam and Rowe
111 2001). PFOA and PFOS are neither hydrophobic or hydrophilic as their surfactant properties
112 results in collecting at interfaces between aqueous and non-aqueous fluids. The $\log K_{ow}$ values for
113 PFOA and PFOS have not been measured experimentally, but various investigators have
114 estimated $\log K_{ow}$ values for these compounds from correlations with other properties of the
115 compound (Arp et al. 2006; Rayne and Forest 2009). The United States Environmental Protection
116 Agency (US EPA) Industry Interface Estimation Suite uses atom/fragment contribution method to
117 estimate $\log K_{ow}$ (US EPA 2012). This computer program predicts $\log K_{ow}$ values of 4.81 (PFOA)
118 and 4.49 (PFOS). This is within the ranges of $\log K_{ow}$ values predicted using other software tools
119 (Arp et al. 2006; Rayne and Forest 2009).

120 Alternative materials are used in conjunction with polyethylene to provide additional diffusive
121 resistance to common landfill leachate contaminants (e.g., BTEX). Ethylene vinyl alcohol
122 (EVOH), a co-polymer of ethylene and vinyl alcohol, is a hydrophilic substance that has high
123 diffusive resistance to gases and organic compounds, such as BTEX and TCE (Lagaron et al.
124 2001; McWatters and Rowe 2014, 2018; Eun et al. 2017). The hydrophilic nature of EVOH results
125 in lower diffusion and partitioning coefficients of non-polar organic contaminants, compared to
126 polyethylene, and geomembranes are being manufactured with EVOH cores coextruded with

127 polyethylene outer layers as mitigation against vapour intrusion (McWatters et al. 2019;
128 McWatters and Rowe 2009, 2010, 2014). This EVOH layer decreases diffusive flux of
129 contaminants through the geomembrane, and inclusion of an 0.0254 mm EVOH layer in a 0.5 mm
130 geomembrane can reduce the steady state flux through a geomembrane for benzene by a factor of
131 19.5, compared to a 1.5 mm HDPE geomembrane (DiBattista and Rowe Forthcoming)

132 The primary objective of this study is to assess the diffusive behaviour of PFOA and PFOS
133 through LLDPE and LLDPE coextruded with EVOH. This information is used to compare the
134 diffusive properties of PFOA and PFOS to other known contaminants of concern.

135 **2. Background**

136 Diffusion is driven by the concentration gradient between two points, and Fick's first law
137 calculates the steady state diffusive flux (f [ML^2T^{-1}]) between two points (z) of a geomembrane for
138 a one-dimensional system (Crank 1979).

$$139 \quad f = -D_g \frac{dc_g}{dz} \quad [1]$$

140 where D_g is the diffusion coefficient of the material [L^2T^{-1}], c_g is geomembrane concentration [ML^{-3}],
141 and c_g [ML^{-3}] is the change in concentration over a small distance, dz [L]. Fick's first law cannot
142 describe the transient aspect diffusion, and Fick's (so called) second law gives the change in
143 concentration with time t .

$$144 \quad \frac{\partial c_g}{\partial t} = D_g \frac{\partial^2 c_g}{\partial z^2} \quad [2]$$

145 Fick's laws are used to calculate diffusion within a geomembrane. However, when the
146 contaminant in is an aqueous solution in contact with the geomembrane, the contaminant
147 undergoes a phase change when partitioning from the aqueous solution (e.g., a source reservoir)
148 into the polymer. This phase change is expressed using the partitioning coefficient S_{gf} (-), which is

149 calculated as the ratio of the geomembrane concentration to the fluid concentration using a
150 modified Henry's Law.

$$151 \quad c_g = S_{gf} c_f \quad [3]$$

152 Under steady state conditions, Eq. 3 can be substituted into Fick's first law such that when there
153 is a constant concentration gradient between the source to receptor equal to the difference in
154 concentration between the two sides of the geomembrane (Δc_f) divided by the geomembrane
155 thickness (H), the mass flux, f , through the geomembrane is given by:

$$156 \quad f = -D_g \frac{dc_g}{dz} = -S_{gf} P_g \frac{dc_f}{dz} = -P_g \frac{\Delta c_f}{H} \quad [4]$$

157 Thus, a permeation coefficient, P_g , can be calculated as the product of D_g and S_{gf} .

158 **3. Materials and Methods**

159 Four geomembranes were used in this study, 0.1 mm LLDPE, 0.1 mm LLDPE coextruded with a
160 0.01 mm layer of EVOH (0.1 mm CoEx), 0.75 mm LLDPE, and 0.75 mm LLDPE coextruded with
161 0.03 mm EVOH (0.75 mm CoEx). Experiments were conducted at room temperature (23°C) and
162 in ovens set at 35°C and 50°C. Cells containing the four geomembranes are currently running at
163 23°C, and elevated temperature testing was initiated for the 0.1 mm LLDPE, 0.75 mm LLDPE,
164 and the 0.75 mm CoEx.

165 Based on Fick's first law, the diffusive flux through a geomembrane is inversely proportional
166 to the membrane thickness. Anticipating that D_g may be low for PFAS and PFOA, the tests were
167 initiated with membranes thinner than the 1.5-3 mm thickness geomembrane typically used in
168 landfill to allow greater diffusion in a shorter time period. The ratio, P_g/H , and the ratio D_g/H can
169 be used to estimate the parameters for thicker geomembranes. Also, HDPE is more commonly
170 used in landfills than LLDPE, but it is known that diffusion coefficient through polyethylene
171 geomembranes generally decreases with higher crystallinity due to a greater tortuosity of the

172 diffusive path through the amorphous zone and around the polyethylene crystals (Islam and Rowe
173 2009). Since LLDPE has a lower crystallinity than HDPE, results from experiments using LLDPE
174 will likely give a conservative estimate for the diffusion coefficients for HDPE (Jones and Rowe
175 2016).

176 Stainless steel double compartment diffusion cells were used in this study. These cells have a
177 source and receptor separated by the geomembrane with volumes of 465 ml (source) and 180 ml
178 (receptor). Similar studies of BTEX diffusion used Viton gaskets to obtain seals between the
179 membrane and the cell (Jones 2016; McWatters 2010; McWatters and Rowe 2018). However, the
180 Viton gaskets, a fluoride copolymer, typically used were replaced with silicone gaskets of the same
181 size to avoid a possible contamination of the cells. Clean cell components were rinsed with 10 ml
182 of 0.1 ammonium hydroxide in methanol; the rinsate concentrations were below detection for
183 PFOA and PFOS.

184 The stock solutions were mixed using 1 g PFOS (97% purity) and 1 g PFOA (98% purity),
185 purchased from Synquest Laboratories (Aluchua, Florida). The PFOA and PFOS were added to 2
186 L and 1 L volumetric flasks with DDI water, respectively, to create separate solutions of 500 mg/L
187 PFOS and 1000 mg/L PFOA. The concentrations of these solutions were analyzed and confirmed.
188 These stock solutions were used to create all source solutions used in the experiments. The
189 diffusion cells had initial source concentrations, c_o , of 19.8 mg/L (PFOA) and 22.7 mg/L (PFOS)
190 to create a large diffusion gradient and increase diffusive flux through the membrane. These
191 concentrations well below the solubility limits at room temperature (2290-4340 mg/L for PFOA
192 and 519-680 mg/L for PFOS) and critical micelle concentration (CMC) of aqueous PFOA
193 (~15,700 mg/L) and PFOS (~4,570 mg/L), and it is unlikely that micelle formation will occur in
194 solution. However, the formation of hemi-micelles can occur in aqueous concentrations as high as

195 0.01-0.001 times the CMC (Johnson et al. 2007; Yu et al. 2008). To assess the impacts of potential
196 hemi-micelle formation on the source concentrations or diffusive processes (if any), additional
197 experiments using the 0.1 mm LLDPE at 23°C, 35°C, and 50°C were initiated with initial PFOA
198 and PFOS concentrations of 1.1 mg/L (below 0.0001CMC for PFOA and 0.001CMC for PFOS).

199 Sampling was performed using separate syringes for the source and receptors to decrease
200 chances of contamination. To sample the cells, a small volume (<200 µl) was removed from the
201 source or receptor and replaced with an equal volume of DDI water. Syringes were then rinsed
202 three times with methanol and DDI water before the next use. Syringe and water blanks were
203 analyzed before experiments began and randomly during the experimental process to ensure results
204 were not influenced by contamination.

205 Sorption experiments using the 0.75 mm LLDPE were also initiated. These experiments were
206 prepared by creating a source solution of 376 ug/L, and this solution was decanted into two vials
207 containing geomembrane and a third control vial with no geomembrane. An initial sample of the
208 solution was extracted before the solution was decanted into the individual vials to confirm initial
209 concentration.

210 All samples were analyzed on an Agilent 6460 LC-MS/MS running in MRM mode.
211 Separation was performed using a 150mm x 2.1mm x 3.0 um Zorbax C18 Eclipse Column
212 coupled with guard column. Samples were eluted over a 10 minute period, starting at 95% water
213 (10 mM ammonium acetate) and 5% acetonitrile, transitioning to 100% acetonitrile over 8
214 minutes, then holding at 100% acetonitrile for the last 2 minutes. The column was then re-
215 equilibrated at original elution conditions for 4 minutes before the next sample analysis.

216 Concentrations were calculated using an eight point calibration curve across 0.01 ug/L to 200
217 ug/L (0.01, 0.1, 1, 5, 10, 50, 100, 200). The varying concentrations of calibration standards were

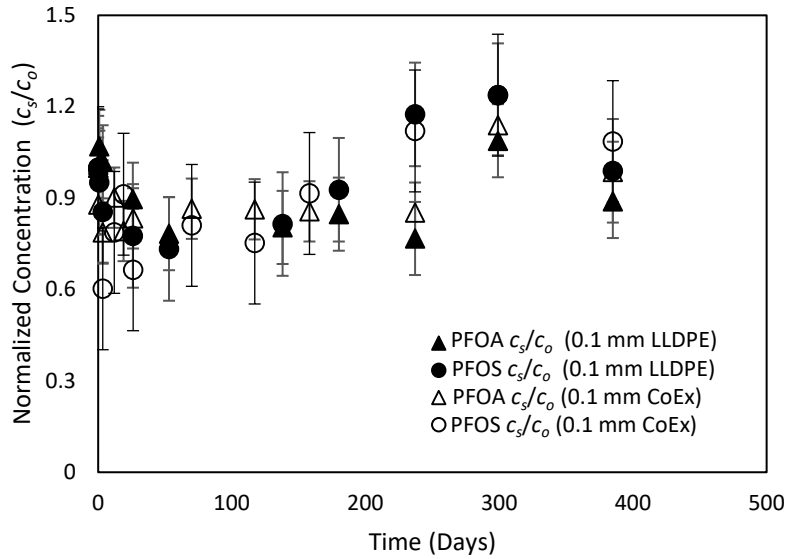
218 made from standards purchased from Wellington Laboratories. Two double injection blanks
219 (methanol) were run before each method blank, reagent blank, calibration curve, post-treatment
220 sample, and experimental blanks to eliminate contamination and carry-over from other samples.
221 The reporting limit for analyses was 0.1 ug/L. Syringe blanks and water blanks were included in
222 the analysis and at sporadic dates throughout the test durations

223 **4. Results**

224 *4.1 Diffusion Testing*

225 Diffusion tests conducted at 23°C for the four geomembranes have sampling data available up to
226 483 days. In this time there has been limited observed permeation of the contaminants through the
227 0.1 mm LLDPE, 0.1 mm CoEx, 0.75 mm LLDPE, and 0.75 mm CoEx. The initial source
228 concentrations for these tests were $c_o=19.8$ mg/L (PFOA) and $c_o=22.7$ mg/L (PFOS). Source
229 concentrations of PFOA and PFOS for the 0.75 mm LLDPE, 0.75 mm CoEx, 0.1 mm LLDPE, and
230 0.1 mm CoEx were scattered about the initial value of the source concentrations (Figure 1), and
231 unlike organic contaminants, there was no pattern of decrease discernable from the scatter over the
232 entire period of monitoring. The scatter requires some explanation. The data over the first 180 days
233 was obtained by analysis from a commercial lab that took no special care (i.e., they were analyzed
234 as routine samples with no additional dilution). These samples had a dilution factor of 15 before
235 being sent for analysis, and the reported concentrations were >10,000 ug/L. The highest point on
236 the calibration curves were 625 ug/L (PFOS) and 312 ug/L (PFOA). Samples analyzed after 180
237 days, were analyzed by a specialized lab, and samples were diluted to fall within the maximum
238 point of the calibration curve (200 ug/L). These samples had high dilution factors (~50), which
239 can magnify any analytical uncertainty. Special attention was paid to obtaining the last data point
240 and it showed minimal decreases and remained close to $c/c_o=1$. The short-term stability in the

241 source concentrations indicate that little to no partitioning of the contaminants to the LLDPE is
242 occurring, and the long-term stability of the source concentrations indicates that minimal diffusion
243 had occurred over the period monitored, as significant mass flux through the geomembrane would
244 notably and consistently decrease the source concentration in the 483-509 days of testing reported
245 herein. The average source concentrations for the cells were 19.5 mg/L ($n=37$, $\sigma=2.5$ mg/L) for
246 PFOA and 24.2 mg/L ($n=36$, $\sigma =5.3$ mg/L), for PFOS. Given the magnitude of the standard
247 deviation, σ , the differences in mean concentrations of the individual cells (LLDPE vs CoEx) were
248 not statistically significant ($p < 0.1$), and the initial concentration was within the 99% confidence
249 intervals calculated for the individual cells. There was no discernible (measurable) decrease in
250 source concentration with time. If the contaminants were partitioning into the geomembrane, as
251 would occur for BTEX or many other organic compounds, or lost to the environment through
252 leakage in the cell gaskets and septa, the individual cell means and population mean would be
253 lower. These conclusions, based on source data alone, are consistent with data from the receptor
254 concentrations and sorption test data for LLDPE discussed below. Although there is uncertainty
255 regarding the precise source concentration, due to the very large difference in source and detected
256 receptor concentrations this uncertainty has a relatively little effect on the diffusion and permeation
257 coefficients, as illustrated later.



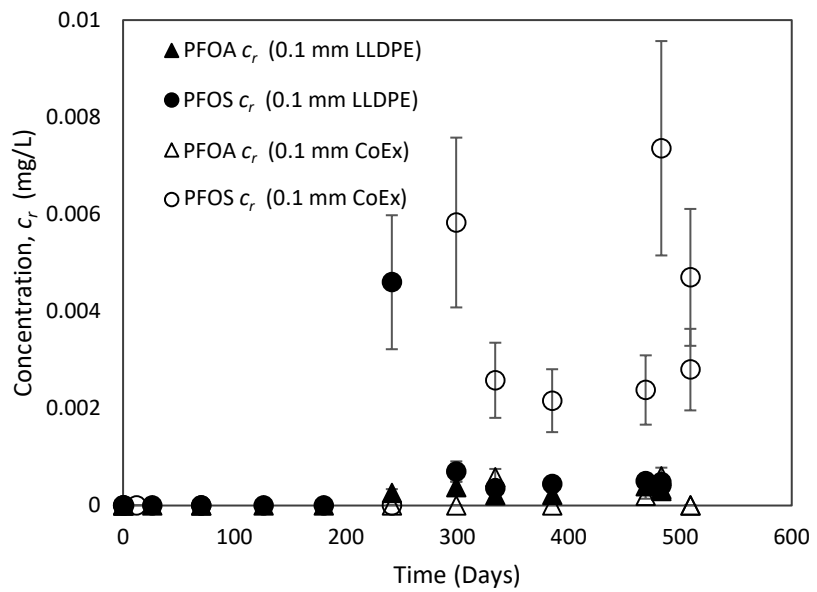
258

259 **Figure 1: Normalized source concentrations, c_s/c_o , for 0.1 mm LLDPE and CoEx at room**
 260 **temperature; $c_o=19.8$ mg/L (PFOA) and $c_o=22.7$ mg/L (PFOS)**

261 Receptor samples had no need for dilution prior to analysis, and the receptor concentrations
 262 will be the primary experimental data used for developing estimates of the diffusion and
 263 permeation coefficients for the materials tested.

264 Excluding the effects of analytical variability and uncertainty, due to a larger diffusion gradient
 265 across the 0.1 mm LLDPE compared to the 0.75 mm LLDPE, contaminant detection for the 23°C
 266 experiments is expected to occur earlier for 0.1 mm geomembranes due to the larger diffusion
 267 gradient compared to the 0.75 mm LLDPE, and at a given time after breakthrough, the
 268 concentration would be greater prior to equilibrium for the 0.1 mm than the 0.75 mm GMB. Also,
 269 if the diffusion coefficient for these compounds is lower for EVOH than LLDPE, detection of
 270 PFOA and PFOS would be expected to occur earlier for LLDPE than for the CoEx of the same
 271 thickness; at a given time after breakthrough, the receptor concentration would be higher prior to
 272 equilibrium. Indeed, the first receptor concentration to exceed the detection limit was the 0.1 mm
 273 LLDPE at 299 days ($c_{PFOA}= 0.4$ ug/L and $c_{PFOS}= 0.7$ ug/L). Receptor concentrations above

274 detection were observed later (at 334 days) for the 0.1 mm CoEx ($c_{PFOA} = 0.6 \text{ ug/L}$ and $c_{PFOS} = 2.6$
 275 ug/L). Even with no dilution, it was found that there was notable scatter in the receptor data and it
 276 is difficult discern a clear trend of increasing concentration with time in the experiments (Figure
 277 2). The concentrations obtained with subsequent sampling for these cells have been very low
 278 ($c_{PFOA} \leq 0.6 \text{ ug/L}$ and $c_{PFOS} \leq 0.8 \text{ ug/L}$) indicating diffusion is occurring extremely slowly. The most
 279 recent sampling data (Supplementary Materials Table S1), at 483 days, had receptor concentrations
 280 of $c_{PFOA} = 0.3 \text{ ug/L}$ and $c_{PFOS} = 0.5 \text{ ug/L}$ (0.1 mm LLDPE) and below detection for both PFOA and
 281 PFOS (0.1 mm CoEx). In comparison, if benzene ($D_g = 2.2 \times 10^{-13} \text{ m}^2/\text{s}$ $S_{gf} = 200$; DiBattista and
 282 Rowe 2020) was the contaminant of interest, an equilibrium would be reached in 31 days ($c_{eq} = 18.9$
 283 mg/L) for the 0.1 mm LLDPE geomembrane using an identical experiment set-up ($c_o = 22 \text{ mg/L}$).



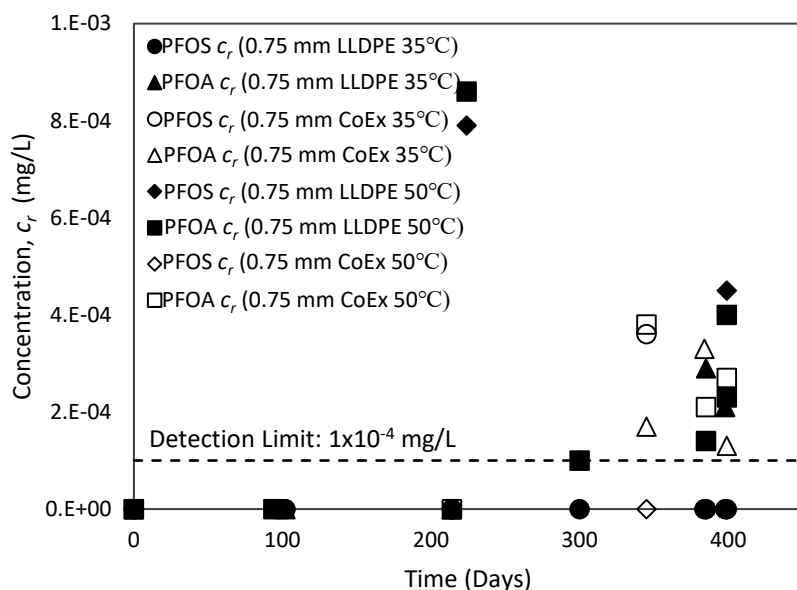
284
 285 **Figure 2: Receptor concentrations, c_r , (detection limit = 0.0001 mg/L) for 0.1 mm LLDPE and 0.1 mm CoEx**
 286 **at 23°C; $c_o = 19.8 \text{ mg/L}$ (PFOA) and $c_o = 22.7 \text{ mg/L}$ (PFOS)**

287 Detection of PFOA in the 0.75 mm LLDPE at 23°C occurred at 299 days (1.4 ug/L), and
 288 detection of PFOS occurred at 429 days (0.3 ug/L). The most recent sampling (509 days) were

289 below detection for PFOA and PFOS; in contrast a diffusion test with $c_o=22.7$ mg/L benzene in an
290 identical cell would reach equilibrium in 77 days ($c_{eq} = 10.3$ mg/L) for 0.75 mm LLDPE. Detection
291 of PFOA in the 0.75 mm CoEx receptor samples occurred at 469 days (0.3 ug/L), and PFOS
292 concentrations have remained below detection for the duration of testing.

293 Permeation of contaminants through geomembranes increases with temperature. Elevated
294 temperature experiments (at 35°C and 50°C) with $c_o=19.8$ mg/L (PFOA) and $c_o=22.7$ mg/L (PFOS)
295 were initiated to assess the effect of temperature on the diffusion of PFOA and PFOS through the
296 0.75 mm LLDPE and CoEx geomembranes, however even at these temperatures very limited
297 permeation of contaminants has been observed in the testing duration. Similar to the 23°C
298 experiments, there has been no discernible depletion in the source concentrations for these elevated
299 temperature tests (e.g., at 50°C in Supplementary Figure S1) with the analyzed concentrations of
300 the 0.75 mm LLDPE experiment at 50°C averaging 22.4 mg/L ($n=7$, $\sigma=2.6$ mg/L) for PFOA
301 ($c_o=19.8$ mg/L) and 27.2 mg/L ($n=7$, $\sigma=5.4$) for PFOS ($c_o=22.1$ mg/L). At the most recent sampling
302 event (399 days), receptor concentrations for the 0.75 mm LLDPE at 50°C were 0.4 ug/L (PFOA)
303 and below quantification (PFOS) and 0.2 ug/L (PFOA) and below quantification (PFOS) at 35°C
304 (Figure 3). The first sampling point above detection occurred at 224 days ($c_{PFOA}= 0.9$ ug/L and
305 $c_{PFOS}= 0.8$ ug/L) for the 50°C test, which is 75 days earlier than observed for the 0.75 mm LLDPE
306 at 23°C while PFOA was detected at 300 days (0.05 ug/L) in the 35°C. PFOS concentrations have
307 been below quantification for this experiment. Faster time to contaminant breakthrough is expected
308 as diffusion will increase as temperature increases (Rowe et al. 2004). Although, the 50°C
309 experiment had contaminant breakthrough sooner, the mass flux through the LLDPE is still
310 extremely low, even at the elevated temperatures, as evidenced by the lack of source depletion and
311 low receptor concentrations at 399 days.

312 The 0.75 mm CoEx geomembrane had receptor concentrations of 0.3 ug/L (PFOA) and below
 313 detection (PFOS) in the 50°C cell, and the 35°C cell had receptor concentrations of 0.1 ug/L
 314 (PFOA) and below detection (PFOS) at 399 days (Figure 3). Receptor PFOA concentrations were
 315 first above detection in the 50°C experiment at 345 days (0.4 ug/L), and PFOS were above
 316 detection but below quantification. The 0.75 mm CoEx at 35°C had receptor detectable receptor
 317 concentrations at 345 days ($c_{PFOA}=0.2$ ug/L and $c_{PFOS}=0.4$ ug/L). Contaminant breakthrough was
 318 observed sooner in the LLDPE tests than in the CoEx tests for the 23°C, 35°C and 50°C tests,
 319 indicating that the EVOH core may provide greater diffusive resistance to PFOA and PFOS
 320 diffusion than the LLDPE.
 321



322
 323 **Figure 3: Receptor concentrations, c_r , for 0.75 mm LLDPE and 0.75 mm CoEx at 50°C; $c_o=19.8$**
 324 **mg/L (PFOA) and $c_o=22.7$ mg/L (PFOS)**

325 The three cells with $c_o=1.1$ mg/L for PFOA and PFOS at 23°C, 35°C, and 50°C have sample
 326 data available up to 202 days. Similar to the experiments using $c_o > 20$ mg/L, the 1.1 mg/L source
 327 concentrations did not exhibit any discernable decreases, and receptor concentrations were below

328 detection for PFOA and PFOS at the 202 day sampling point. Similar observed behaviour in the
329 source of $c_o=1.1$ mg/L and $c_o > 20$ mg/L indicate that hemi-micelle formation on the cell walls or
330 geomembrane surface (if present) is not discernably affecting the initial stages of diffusion through
331 the geomembrane, however these tests will remain active for future monitoring.

332 *4.2 Room Temperature Sorption Testing*

333 Sorption tests were conducted with LLDPE at 23°C with $c_o=263$ ug/L for both PFOA and PFOS
334 ($c_o < 0.0001$ CMC); a control test with no geomembrane was also assembled at the same time. These
335 tests have been active for 226 days, and there have been small decreases in PFOA and PFOS
336 concentrations observed in the vials containing the LLDPE compared to the control vial. Using
337 the mass balance of the sorption tests, S_{gf} can be calculated from

$$338 \quad S_{gf} = \frac{[c_{fo}V_{fo} - c_{fF}V_{fF} - M_c]\rho_g}{M_g c_{gF}} \quad [5]$$

339 where c_{fo} , c_{fF} , c_{gF} denote initial and final aqueous concentrations and the final concentration of the
340 geomembrane at equilibrium [ML^{-3}], respectively, and V_{fo} and V_{fF} denote initial and final solution
341 volumes [L^3]. The geomembrane mass and mass of contaminant lost to the system (quantified
342 using control tests) are expressed as M_g and M_c [M], respectively, and geomembrane density is
343 denoted as ρ_g [L^3M].

344 Using Eq. 5, estimates of the partitioning coefficients were calculated: 0.9-1.4 (PFOA) and 2.8-
345 5.3 (PFOS). These preliminary S_{gf} values support the limited source decreases observed in the
346 diffusion experiments for $c_o > 20$ mg/L and $c_o = 1.1$ mg/L. These values are currently the best
347 estimates, however despite the fact that these tests have been running a relatively long time, it is
348 unlikely that they have reached equilibrium during the period of observation due the low
349 diffusivity of PFOA and PFOS through LLDPE, as observed in the diffusion experiments.
350 Monitoring of these experiments is ongoing.

351 4.3 Preliminary Diffusion Modelling

352 Using a the finite layer program POLLUTE v7(Rowe and Booker 1985, 2004, Rowe et al. 1988,
353 1997; Barone et al. 1990, 1992a;b; ; Rowe and Badv 1996; Rowe 1998; Lake and Rowe 2004;
354 Sangam and Rowe 2001; Rowe et al. 2005), best estimate diffusion coefficients were developed
355 for LLDPE by modelling the receptor concentrations with time for the diffusion experiments. The
356 D_g values were developed by matching a theoretical model to the receptor concentrations at the
357 most recent sampling event. If receptor concentrations were below detection or quantification,
358 such that no number could be assigned from the test, a concentration equal to the detection (0.1
359 ug/L) concentration was used to obtain an upper bound on the diffusion coefficient for the value
360 of S_{gf} inferred from the sorption test. Best estimate diffusion coefficients and consequent
361 partitioning coefficients were inferred from the latest data point given the absence of any clear
362 trend of an increase with time (Table 1), however the receptor concentrations are extremely low
363 for all tests (< 8 ug/L, $c_r/c_o < 0.0004$), and the diffusion/permeation coefficients reported may
364 decrease further with the availability of new data and more time. For PFOA diffusing through 0.1
365 mm LLDPE, the best estimate is $D_g \leq 2.5 \times 10^{-17}$ m²/s and $P_g \leq 3.1 \times 10^{-17}$ m²/s and for PFOS the
366 best estimate is $D_g \leq 4.0 \times 10^{-17}$ m²/s and $P_g \leq 1.6 \times 10^{-16}$ m²/s after 483 days at 23°C.

367 The 23°C partitioning coefficients were used to model the elevated temperature tests although
368 the partitioning coefficients are likely to increase with temperature, however, the limited
369 reductions in source concentrations for the tests at 35°C and 50°C indicate that there is limited
370 contaminant partitioning occurring, even at the elevated temperatures. Preliminary best estimate
371 diffusion coefficients have been proposed for the LLDPE at 23°C, 35°C, and 50°C (Table 1). To
372 illustrate the value of running tests longer, especially when receptor concentrations are below or
373 near the detection limit, one can compare best estimates for P_g obtained from the 50°C 0.75 mm

374 LLDPE experiments; at 214 days, the best estimate $P_g \geq 3.8 \times 10^{-15}$ m²/s compared to $P_g > 1.4$ -
375 1.9×10^{-15} m²/s at 399 days, for PFOA and note the decrease by a factor of two. Due to the preliminary
376 nature of these results (only 399 days testing at 35 and 50°C) with the receptor concentrations near
377 or below detection, no clear trend is evident in an Arrhenius plot of the natural logarithm of the
378 best estimate permeation coefficients, P_g , plotted against the inverse of temperature (in K), $1/T$,
379 for the 0.75 mm LLDPE and CoEx membranes (Figure S2). LLDPE is an effective barrier to PFOA
380 and PFOS, as evidenced by P_g values for LLDPE ranging from $\leq 5.2 \times 10^{-15}$ m²/s (PFOS at 50°C)
381 to as low as $\leq 3.1 \times 10^{-17}$ m²/s (PFOA at 23°C).

382 The 0.1 mm material was tested because, for the same source and receptor properties and initial
383 source concentrations, a contaminant diffusing through geomembranes of the same material but
384 different thickness, will reach the receptor earlier for the thinner geomembrane. This is why the
385 best estimate values reported for the 0.1 mm and the 0.75 mm LLDPE vary by more than an order
386 of magnitude. Despite 509 days of testing, receptor concentrations for the 0.75 mm LLDPE were
387 below detection or quantification (Supplementary Materials Table S1). Thus, the P_g value has to
388 be estimated based on the detection limit at 509 days. The longer the test is run and the receptor
389 remains below the detection limit, the lower will be the estimate of P_g . Once the sampled receptor
390 concentrations for the 0.1 mm and 0.75 mm LLDPE are consistently above the detection levels
391 and there is a trend of increasing receptor concentration with time, the best estimate P_g for the 0.75
392 mm LLDPE will likely be similar to the values reported for the 0.1 mm LLDPE. That said, the P_g
393 values for the 0.75 mm LLDPE (Table 1) are still very low. Nevertheless, as the 0.1 mm LLDPE
394 experiments had more data points above detection during the monitoring period they are
395 considered more representative of the actual P_g and so the following comparisons and discussion
396 will be based on the best estimates provided for the 0.1 mm LLDPE.

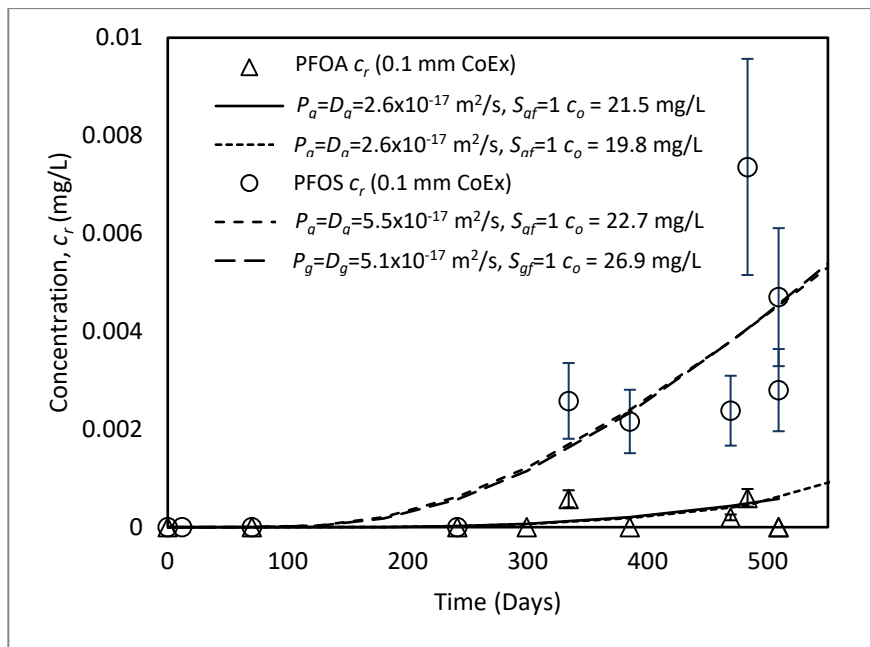
397 **Table 1: PFOA and PFOS best estimate D_g , S_{gf} , and P_g values for LLDPE and CoEx**
 398 **membranes at multiple temperatures**

Material	PFOA			PFOS			
	Temp. (°C)	D_g ($\times 10^{-16} \text{m}^2/\text{s}$)	S_{gf} (-)	P_g ($\times 10^{-16} \text{m}^2/\text{s}$)	D_g ($\times 10^{-16} \text{m}^2/\text{s}$)	S_{gf} (-)	P_g ($\times 10^{-16} \text{m}^2/\text{s}$)
0.1 mm LLDPE	23	≤ 0.25	0.9-1.4	≤ 0.31	≤ 0.40	2.8-5.3	≤ 1.6
0.75 mm LLDPE	23	≤ 10	0.9-1.4	$\leq 9-13$	$\leq 6.5-6.7$	2.8-5.3	$\leq 19-34$
0.75 mm LLDPE	35	$\leq 9.3-10$	0.9-1.4	$\leq 9-13$	$\leq 7.6-7.8$	2.8-5.3	$\leq 22-40$
0.75 mm LLDPE	50	$\leq 10-19$	0.9-1.4	$\leq 14-19$	$\leq 9.8-9.9$	2.8-5.3	$\leq 27-52$
0.1 mm CoEx	23	-	-	≤ 0.26	-	-	≤ 0.55
0.75 mm CoEx	23	-	-	≤ 8.6	-	-	≤ 6.8
0.75 mm CoEx	35	-	-	≤ 11	-	-	≤ 8.3
0.75 mm CoEx	50	-	-	≤ 10	-	-	≤ 8.2

399 Using the same a method to deduce D_g values for LLDPE, best estimate P_g values are proposed
 400 for the coextruded membranes based on the experiments 23°C, 35°C, and 50°C (Table 1). Since
 401 there is no data available regarding diffusion of PFOA and PFOS through individual components
 402 of the system S_{gf} and D_g cannot be defined for the system. At 23°C, best estimate P_g values for are
 403 $P_{gPFOA} \leq 2.6 \times 10^{-17} \text{ m}^2/\text{s}$ and $P_{gPFOS} \leq 5.5 \times 10^{-17} \text{ m}^2/\text{s}$ for the 0.1 mm CoEx (Figure 4) and P_{gPFOA}
 404 $\leq 8.6 \times 10^{-16} \text{ m}^2/\text{s}$ (PFOA) and $P_{gPFOS} \leq 6.8 \times 10^{-16} \text{ m}^2/\text{s}$ (PFOS) for the 0.75 mm CoEx. The proposed
 405 parameters are current best estimates based on the limited receptor data arising from the
 406 remarkably low receptor concentrations despite relatively high values of $c_o = 19.8 \text{ mg/L}$ and $c_o =$
 407 22.7 mg/L . To assess the effect of uncertainly due to the variability observed in the experimental
 408 data, P_g was also obtained by modelling the data for c_o values representative of the later time source
 409 data (i.e., $c_o = 21.5 \text{ mg/L}$ for PFOA and $c_o = 26.9 \text{ mg/L}$ for PFOS; Figure 4), and the deduced
 410 values of P_g were not notably different from the original best estimates and the higher c_o actually
 411 results in a lower estimate of P_g .

412 Best estimate P_g values for the 0.75 mm CoEx ranged from $\leq 6.8 \times 10^{-16}$ m²/s (PFOS 23 °C) to
 413 $\leq 1.1 \times 10^{-15}$ m²/s (PFOA 35 °C). These values are based on the data available, and the proposed
 414 best estimates are likely to decrease as monitoring continues. Upper bound permeation coefficients
 415 could be developed such that the modelled concentrations match the date and concentration of the
 416 maximum analyzed concentration. This would be very conservative as, generally, the receptor
 417 concentrations have been oscillating above and below the detection limit for most cells. The
 418 estimated vales of P_g are likely to decrease as the test runs for a longer period of time, and will be
 419 more clearly defined when concentrations in the receptor are consistently above the detection limit
 420 and show a clear trend of increasing with time. For comparable thicknesses, the CoEx consistently
 421 has similar or lower P_g values than the LLDPE alone.

422



423

424 **Figure 4: PFOA Observed and calculated receptor concentrations, c_r , for 0.1 mm CoEx for**
 425 **both PFOA and PFOS at 23°C. Two calculated curves are shown for each. One is for the**
 426 **initial source concentration ($c_o= 19.8$ mg/L for PFOA and $c_o=22.7$ mg/L for PFOS) and the**

427 **other for a representative value in the latter part of the test ($c_o= 21.5$ mg/L for PFOA and**
428 **$c_o=26.9$ mg/L for PFOS).**

429 **5. Discussion**

430 The best estimate parameters for the LLDPE and the coextruded geomembranes can be compared
431 to diffusion parameters for polyethylene that have been proposed for a variety of contaminants that
432 exist in landfill leachate (Table 2). Organic contaminants, specifically BTEX, have greater D_g , S_{gf} ,
433 and P_g values for LLDPE than PFOA and PFOS; this is, in part, likely due to smaller molecular
434 weights, M_w , and greater hydrophobicity, of the BTEX compounds compared to PFOA and PFOS.
435 Although the estimated $\log K_{ow}$ values for PFOA and PFOS are higher than those of BTEX (Table
436 2), their molecular structures result in molecules that have both lipophilic and hydrophilic
437 properties, and the hydrophilic functional end groups are likely to decrease the ability of the
438 contaminant to partition from an aqueous phase solution to the LLDPE (Rayne and Forest 2009).
439 Studies of other emerging contaminants with $M_w > M_{wBTEX}$ have shown that polybrominated
440 diphenyl ethers (PBDE) and polychlorinated biphenyl Aroclor 1242 (PCBs)s have extremely high
441 S_{gf} values (>150,000) for HDPE, resulting in P_g values greater than the P_g values for BTEX, and
442 S_{gf} values more than 30,000-fold greater than best estimates calculated for PFOA and PFOS (Table
443 2 and Rowe et al. 2016b; a). This is likely influenced by other chemical properties beside M_w , such
444 as hydrophobicity. Bisphenol-A (BPA) and phenol are emerging contaminants that behave in a
445 more similar manner to PFOA and PFOS, where little to no partitioning of the BPA and phenol
446 into HDPE was observed, even though the calculated $\log K_{ow}$ value for BPA is greater than those
447 of BTEX and its solubility is similar to or lower than BTEX (Supplementary Material Table S2)
448 BPA has a very low S_{gf} value, and, over 1500 days of monitoring, there was limited source
449 concentration decrease and receptor concentration increase for BPA (Saheli et al. 2016). When
450 comparing the M_w of contaminants to their respective D_g values for polyethylene, PFOA and PFOS

451 follow a similar trend as BTEX, PCBs, PBDE, BPA, and phenol and their respective D_g values for
 452 polyethylene (Figure 5); as M_w increases, D_g decreases in an exponential fashion. The solubility of
 453 BPA (120-380 mg/L) with $S_{gf} \leq 1$ (too small to be measured reliably) and phenol (90,000 mg/L)
 454 with $S_{gf} \sim 3.5$ bracket those for PFOA (2290-4340 mg/L) and PFOS (519-680 mg/L;
 455 Supplementary Material Table S2) and so to the extent S_{gf} is related to solubility one would expect
 456 $1 \leq S_{gf} \leq 3.5$ for PFOA and PFAS; however S_{gf} depends on more than solubility. The topological
 457 polar surface areas [\hat{A}^2], a measure of surface area in a molecule from polar atoms, ranged from
 458 20.2 \hat{A}^2 (phenol) to 62.8 \hat{A}^2 (PFOS). When compared with compounds with higher S_{gf} values,
 459 BTEX and PCBs have a topological surface area of 0 \hat{A}^2 while PBDE, which has $S_{gf}=1,800,000$,
 460 has a topological surface area of 9.2 \hat{A}^2 . Thus, while the polar surface area may be a contributing
 461 factor to the ability of a compound to partition to polyethylene, it too is unlikely to be the main
 462 predictor, based on the PBDE values. These complexities make it difficult to develop simple
 463 empirical relationships to predict S_{gf} as will be shown later.

464 **Table 2: PFOA and PFOS best estimate D_g , S_{gf} , and P_g values compared to literature values**
 465 **for other chemicals at room temperature**

Contaminant	$\log K_{ow}$	M_w	D_g	S_{gf}	P_g
	(-)	(g/mol)	(m ² /s)	(-)	(m ² /s)
PFOA – CoEx 0.1 mm	4.81 ^e	414.07	-	-	<2.6x10 ⁻¹⁷
PFOS – CoEx 0.1 mm	4.49 ^e	500.13			<5.5x10 ⁻¹⁷
PFOA – LLDPE 0.1 mm	4.81 ^e	414.07	<2.5x10 ⁻¹⁷	0.9-1.4	<3.1x10 ⁻¹⁷
PFOS – LLDPE 0.1 mm	4.49 ^e	500.13	<4x10 ⁻¹⁷	2.8-5.3	<1.6x10 ⁻¹⁶
Benzene ^a	2.15 ^f	78.11	2.2x10 ⁻¹³	200	4.4x10 ⁻¹¹
Toluene ^a	2.73 ^f	92.14	2.2x10 ⁻¹³	350	7.7x10 ⁻¹¹
Ethylbenzene ^a	3.15 ^f	106.17	1.0x10 ⁻¹³	925	9.2x10 ⁻¹¹
<i>m&p</i> -Xylene ^a	3.15-3.2 ^f	106.16	0.8x10 ⁻¹³	900	7.2x10 ⁻¹¹
<i>o</i> -xylene ^a	3.16 ^f	106.16	0.8x10 ⁻¹³	900	7.2x10 ⁻¹¹
PCBs Aroclor 1242 ^b	6.98 ^e	291.98	5-50x10 ⁻¹⁵	90,000-325,000	0.45-16x10 ⁻⁹

BPA ^c	3.64 ^e	228.29	-	-	2.9x10 ⁻¹⁵
Phenol ^c	1.46 ^c	94.11	1.7x10 ⁻¹⁴	3.48	5.9x10 ⁻¹⁴
PBDE (DE-71 Mixture) ^d	6.81-7.90 ^d	564.7	4x10 ⁻¹⁵	1,800,000	7.2x10 ⁻⁹

^aLLDPE (DiBattista and Rowe 2019)

^bHDPE (Rowe et al. 2016a)

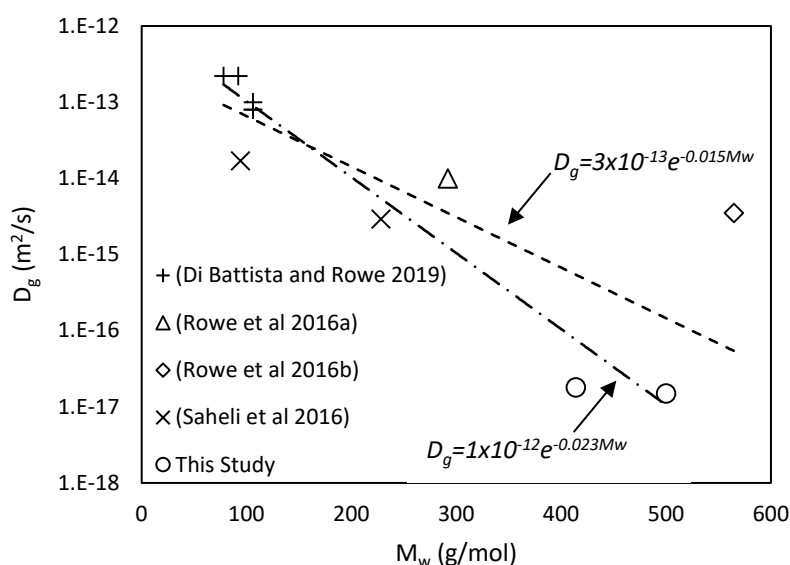
^cHDPE (Saheli et al. 2016)

^dHDPE (Rowe et al. 2016b)

^eCalculated using US EPA Industry Interface Estimation Suite (US EPA 2012)

^f(Montgomery and Welkom 1989)

466



467

468 **Figure 5: Diffusion coefficient variation with molecular weight for various contaminants**
 469 **from this study and previous studies**

470 Prior to this study, there was no available information regarding the diffusion parameters of
 471 PFOA and PFOS for polyethylene, but estimations for D_g , S_{gf} , and P_g could be calculated using
 472 correlations from the literature. Sangam and Rowe (2001) developed the following correlations
 473 using M_w , and $\log K_{ow}$ of organic contaminants to predict the P_g , D_g , and S_{gf} values for HDPE:

474
$$\log S_{gf} = -1.1523 + 1.2355(\log K_{ow}) \quad [R1]$$

475
$$\log P_g = -13.4476 + 2.2437(\log K_{ow}) - 0.3910(\log K_{ow})^2 \quad [R2]$$

476 $\log P_g = -25.6933 + 0.2633M_W - 1.0995 \times 10^{-3}(M_W)^2$ [R3]

477 $\log D_g = -12.3624 + 0.9205\log K_{ow} - 0.3424(\log K_{ow})^2$ [R4]

478 These correlations were developed using semi-empirical and empirical methods for
 479 contaminants with an affinity for polyethylene. Using Eqs. R1, R2, R3, and R4, D_g , S_{gf} , and
 480 P_g values can be calculated based on the contaminant properties of PFOA and PFOS and compared
 481 to the best estimate D_g , S_{gf} , and P_g values deduced from this study (Table 3). The authors recognize
 482 that the correlations were developed for contaminants with a high affinity for polyethylene using
 483 parameters reported for HDPE instead of LLDPE, and that the empirical predictions based on
 484 polymer class do not account for geomembrane specific factors affecting diffusion, (e.g.
 485 crystallinity within the range relevant to a class).

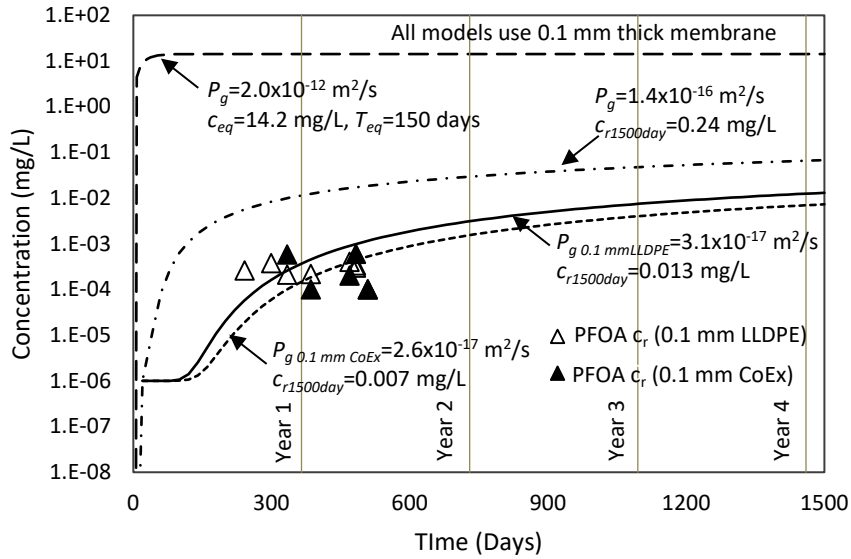
486 **Table 3: Comparison PFOA and PFOS best estimate D_g , S_{gf} , and P_g values LLDPE to**
 487 **values calculated using relationships presented by Sangam and Rowe (2001)**

	PFOA	PFOS
D_g (This study)	$<2.5 \times 10^{-17}$ m ² /s	$<4 \times 10^{-17}$ m ² /s
S_{gf} (This study)	0.9-1.4	2.8-5.3
P_g (This study)	$<3.1 \times 10^{-17}$ m ² /s	$<1.6 \times 10^{-16}$ m ² /s
[R1] $\log S_{gf} = -1.1523 + 1.2355(\log K_{ow})$	$S_{gf}=61,000$	$S_{gf}=25,000$
[R2] $\log P_g = -13.4476 + 2.2437(\log K_{ow}) - 0.3910(\log K_{ow})^2$	$P_g=2.0 \times 10^{-12}$ m ² /s	$P_g=5.5 \times 10^{-12}$ m ² /s
[R3] $\log P_g = -25.6933 + 0.2633M_W - 1.0995 \times 10^{-3}(M_W)^2$	$P_g=6.6 \times 10^{-106}$ m ² /s	$P_g=9.4 \times 10^{-170}$ m ² /s
[R4] $\log D_g = -12.3624 + 0.9205\log K_{ow} - 0.3424(\log K_{ow})^2$	$D_g=1.4 \times 10^{-16}$ m ² /s	$D_g=7.4 \times 10^{-16}$ m ² /s

488 The S_{gf} values calculated using Eq. R1 (61,000 for PFOA and 25,000 for PFOS) are many orders
 489 of magnitude greater than the best estimates calculated using the experimental data. These values
 490 are high, like the S_{gf} values calculated for PCBs ($S_{gf} = 90,000$) and PBDE ($S_{gf} = 1,800,000$), and
 491 would have resulted in rapid depletion of the source concentrations if true for PFOA and PFOS

492 (Rowe et al. 2016b; a). Since no discernible source depletion was observed in all tests, Eq. R1
493 using $\log K_{ow}$ is not a suitable predictor of S_{gf} for PFOA and PFOS.

494 Eqs. R2 and R3 are correlations to calculate P_g using M_w and $\log K_{ow}$, respectively. Values
495 predicted by Eq. R2 (2.0×10^{-12} m²/s for PFOA and 5.5×10^{-12} m²/s for PFOS) are comparable to P_g
496 values reported for BTEX. Modelling of PFOA diffusion through the LLDPE geomembrane using
497 POLLUTE and the P_g values calculated from Eqs. R2 and R3 overpredicts the experimental
498 observations. PFOA modelling using the $P_g = 2.0 \times 10^{-12}$ m²/s, calculated from Eq. R2, predicted
499 that the PFOA source and receptor concentrations would reach equilibrium at approximately 150
500 days (Figure 6). Similarly using $P_g = 5.5 \times 10^{-12}$ m²/s from Eq. 2 for PFOS would predict that
501 concentrations would reach equilibrium at approximately 60 days. However, in reality there was
502 no measurable change in the source concentration of either PFOA or PFOS and barely detectable
503 concentrations in the receptor after 483 days and hence the predicted values from R2 are not
504 correct. At the other extreme, Eq. R3 gives $P_g = 6.5 \times 10^{-106}$ m²/s (PFOA) and $P_g = 9.4 \times 10^{-170}$ m²/s
505 (PFOS). These P_g values are more than 90 orders of magnitude lower than those calculated using
506 Eq. R2. POLLUTE modelling of the experiments using $P_g = 6.5 \times 10^{-106}$ m²/s ($P_g = D_g$, $S_{gf} = 1$) for
507 PFOA ($c_o = 19.8$ mg/L) and $P_g = 9.4 \times 10^{-170}$ m²/s ($P_g = D_g$, $S_{gf} = 1$) for PFOS ($c_o = 22.7$ mg/L), predicts
508 receptor concentrations of $< 10^{-48}$ mg/L for both contaminants at 1500 days. Since PFOA and PFOS
509 have been detected in the receptors before and at 483 days, these values cannot be even close.



510

511 **Figure 6: Experimental PFOA concentrations for 0.1 mm LLDPE and 0.1 mm CoEx, and**
 512 **predicted PFOA receptor concentrations for $D_g=2.5 \times 10^{-17} \text{ m}^2/\text{s}$ $S_{gf}=1.4$ $P_g=3.1 \times 10^{-17} \text{ m}^2/\text{s}$**
 513 **(0.1 mm LLDPE), $D_g=P_g=2.6 \times 10^{-17} \text{ m}^2/\text{s}$ $S_{gf}=1$ (0.1 mm CoEx), $P_g=D_g=2.0 \times 10^{-12} \text{ m}^2/\text{s}$ [Eq.**
 514 **R2], and $P_g=D_g=1.4 \times 10^{-16} \text{ m}^2/\text{s}$ [Eq. R4]. Predicted receptor concentration for $P_g=6.6 \times 10^{-106}$**
 515 **m^2/s (Eq. R3)at 1500 days is $<1 \times 10^{-48} \text{ mg/L}$ and is not shown.**

516 Eq. R4, gave $D_g=1.4 \times 10^{-16} \text{ m}^2/\text{s}$ (PFOA) and $D_g=7.4 \times 10^{-16} \text{ m}^2/\text{s}$ (PFOS) based on the
 517 compounds' $\log K_{ow}$. These values are the closest to the best estimates deduced from the
 518 experiments compared to the P_g and S_{gf} values calculated using Eqs. R1, R2, and R3. POLLUTE
 519 modelling of the experiment using $D_g=1.4 \times 10^{-16} \text{ m}^2/\text{s}$ (PFOA; $P_g=D_g$, $S_{gf}=1$), Figure 6, and
 520 $D_g=7.4 \times 10^{-16} \text{ m}^2/\text{s}$ (PFOS; $P_g=D_g$, $S_{gf}=1$) predicted receptor concentrations of 87 ug/L (PFOA) and
 521 138 ug/L (PFOS) at 483 days, compared to the analyzed concentrations of 0.3 ug/L (PFOA) and
 522 0.5 ug/L (PFOS). Thus, the parameters estimated with this approach are quite conservative and
 523 over predict the observed receptor concentrations by more than two orders of magnitude at 483
 524 days. A value of $S_{gf} = 1$ was used when modelling using the D_g calculated from Eq. R4 because
 525 the S_{gf} predicted by Eq. R1 was too high to be applicable.

526 The modelling of the experiments using the current best estimates of $P_{gPFOA} = 3.1 \times 10^{-17} \text{ m}^2/\text{s}$
527 and $P_{gPFOS} = 1.6 \times 10^{-16} \text{ m}^2/\text{s}$ predicted receptor concentrations of the 0.1 mm LLDPE at 23°C, at
528 1500 days, will be 8.0 ug/L for PFOA ($c_o = 19.8 \text{ mg/L}$; $c/c_o = 4 \times 10^{-4}$) (Figure 6) and 57.6 ug/L (PFOS
529 $c_o = 22.7 \text{ mg/L}$; $c/c_o = 2.5 \times 10^{-3}$). Predicted receptor values using R2, R3, and R4 for PFOA and PFOS
530 at 483 days are given in Supplementary Material Table S3 for 0.1 mm LLDPE.

531 The authors hypothesize that the low permeation of PFOA and PFOS is related to the molecular
532 weight, acidic nature, and surfactant properties of the contaminants. The molecular weights of the
533 contaminants are 414.07 g/mol (PFOA) and 500.13 g/mol (PFOS), which are greater than the
534 molecular weights of BTEX (78.11-106.16 g/mol), PCBs (291.98 g/mol), BPA (228.29 g/mol),
535 and phenol (94.11 g/mol) and comparable to PBDE (564.7 g/mol). The estimated P_g of PBDE is
536 $7.2 \times 10^{-9} \text{ m}^2/\text{s}$, however it is difficult to directly compare the diffusion behaviour of PFOA and
537 PFOS to PBDE as the extremely high partitioning coefficient controls the P_g . PFOA and PFOS are
538 considered very strong acids, and the compounds have estimated pK_a values of -0.2 (PFOA) and -
539 3.3 (PFOS) (Deng et al. 2012). The aqueous source pH ($c_o \sim 20 \text{ mg/L}$) ranged from 3.83-4.05, as
540 measured using a pH probe, and the PFOA and PFOS are likely to be in a dissociated form in these
541 tests and in the environment, as reported pH values in landfill leachate range from 5.9-8.5 in
542 municipal solid waste (Bonaparte et al. 2002; Rowe et al. 2004). Limited partitioning of PFOA
543 and PFOS due to their acidic nature is consistent with experiments using acetic acid with
544 polypropylene and polyethylene membranes, where negligible sorption of the acetic acid to the
545 geomembranes was observed (Aminabhavi and Naik 1998). The surfactant properties of these
546 contaminants result in hydrophilic and lipophilic characteristics; the hydrophilic nature of these
547 contaminants could be a possible explanation for the low partitioning of the contaminants from an
548 aqueous solution into the geomembrane.

549 As discussed, the LLDPE (and likely HDPE) and CoEx geomembranes are both extremely
550 effective diffusive barriers to PFOA and PFOS. However, landfill leachates contain a variety of
551 hydrocarbons, such as BTEX, in addition to PFAS, and polyethylene has lower diffusive resistance
552 to BTEX than geomembranes coextruded with EVOH that have a P_g orders of magnitude lower
553 than for LLDPE (DiBattista and Rowe 2020; Eun et al. 2017; Jones and Rowe 2016; McWatters
554 and Rowe 2010, 2018; Rowe et al. 2004). In addition to low permeation of PFOA and PFOS,
555 membranes coextruded with EVOH have the benefit of additional superior diffusive resistance to
556 other contaminants, like BTEX, found in landfill leachates.

557 **6. Conclusions**

558 Diffusion and partitioning of PFOA and PFOS with respect to LLDPE and LLDPE coextruded
559 with EVOH was investigated for concentrations above and below 0.001 CMC at 23°C, 35°C, and
560 50°C using diffusion testing and sorption vial testing (LLDPE only). The following conclusions
561 were developed; these conclusions are preliminary as only very low concentrations and no
562 consistent trend were detected throughout the 509 day monitoring period. For the materials and
563 conditions tested, these preliminary conclusions are:

- 564 1. Testing demonstrated very limited diffusion through both the coextruded geomembranes
565 with an EVOH core and the LLDPE geomembranes. While both types of membranes
566 exhibit low diffusivity of PFOA and PFOS, the coextruded geomembranes with an EVOH
567 core (CoEx) performed better in all test where a direct comparison could be made while,
568 the literature also shows that the coextruded geomembranes with an EVOH core has the
569 added benefit of being a superior barrier to organic contaminants (e.g., BTEX) present in
570 landfill leachate.

- 571 2. It is unlikely that hemi-micelle and micelle formation, if present, affected the diffusion
572 properties of the membranes, as similar behaviour was observed in experiments with $c_o >$
573 20 mg/L and $c_o = 1.1$ mg/L.
- 574 3. Results from the sorption test vials indicated limited partitioning of contaminants to
575 LLDPE, and S_{gf} values of 0.9-1.4 (PFOA) and 2.8-5.3 (PFOS) were calculated from these
576 tests. Diffusion experiments did not exhibit detectable decreases in source concentration,
577 confirming that minimal partitioning of the contaminants to the polyethylene is occurring
578 and consistent with theoretical predictions based on the best estimate diffusion and
579 permeation parameters.
- 580 4. At the last sampling event before writing this paper, receptor contaminant concentrations
581 were 0.3 ug/L (PFOA) and 0.5 ug/L (PFOS) for the 23°C 0.1 mm LLDPE (483 days) and
582 below detection for PFOA and 3.7 ug/L for PFOS for the 0.1 mm CoEx (at 509 days). This
583 resulted in best estimates of P_g of $\leq 3.1 \times 10^{-17}$ m²/s (PFOA) and $\leq 1.6 \times 10^{-16}$ m²/s (PFOS)
584 for LLDPE and P_g values of $\leq 2.6 \times 10^{-17}$ m²/s (PFOA) and $\leq 5.5 \times 10^{-17}$ m²/s (PFOS) for the
585 0.1 mm CoEx. These values have been deduced using the data available, and it is likely
586 that they will be further refined with time. Permeation coefficient, P_g values deduced for
587 the 0.75 mm LLDPE at various temperatures ranged from $\leq 6.8 \times 10^{-16}$ m²/s (PFOS, 0.75 mm
588 CoEx at 23°C) to $\leq 5.2 \times 10^{-15}$ m²/s (PFOS, 0.75 mm LLDPE at 50°C).
- 589 5. When compared to existing diffusion and partitioning coefficient estimates of BTEX,
590 PBDE, BPA, and PCBs, the diffusion of PFOA and PFOS is most comparable to BPA,
591 where limited partitioning and diffusion through the membranes was observed during the
592 monitoring. Relationships to predict D_g , S_{gf} , and P_g , as proposed by Sangam and Rowe
593 (2001) do not adequately capture the behaviour of PFOA and PFOS. It is likely that the

594 high molecular weights and surfactant nature of these molecules result in extremely low P_g
595 values for LLDPE.

596 For landfills containing PFOA and PFOS as well as volatile organic contaminants (*e.g.*, BTEX,
597 TCE, PCE etc.) that could impact groundwater by diffusion through an unsaturated zone between
598 a single GMB/GCL composite liner and an aquifer, an overarching conclusion is that by the use
599 of a co-extruded 1.5 mm GMB with an EVOH core (as has been used to contain hydrocarbon
600 contaminated soil in Antarctica; McWatters et al. 2016) deserves more consideration than it has
601 been given in the past.

602 These conclusions are specific to diffusive contaminant transport only and are based on the data
603 available. These conclusions do not account for other factors that may affect contaminant transport
604 through geomembranes (*e.g.*, holes in the geomembrane, aging etc.)

605 This study did not consider the depletion of antioxidants from, or the effect of the PFAS on, the
606 service-life of the either the LLDPE or coextruded geomembranes. Aging studies of HDPE using
607 leachate constituents found that the presence of surfactants in the leachate resulted in reductions
608 of standard and high pressure oxidative inductive times as the geomembrane aged (Abdelaal et al.
609 2014). If the surfactant properties of PFOA and PFOS result in similar antioxidant depletion, an
610 additional benefit of geomembranes with coextruded EVOH cores could be protection of the
611 receptor facing polyethylene from antioxidant depletion. This is a hypothesis that requires
612 additional experimentation and study to confirm.

613

614 **Acknowledgements**

615 This study is was financially supported by Kuraray America Inc., who also provided materials for
616 testing, and the authors are grateful for their support. Additionally, the authors would like to thank

617 Dr. A. Rutter and the Analytical Services Unit at Queen’s University, for their support and use of
618 laboratory facilities.

619 Data Availability Statement: The data used during the study is available from the first author upon
620 request, and models used in analysis is commercially available from GAEA Technologies Ltd.

621 Supplemental material: Tables S1-S3 and Figures S1-S2 are available with the online version of
622 the journal article.

623 **References**

624 3M Company. (1999a). *The Science of Organic Fluorochemistry*.

625 3M Company. (1999b). *Fluorochemical Use, Distribution and Release Overview*.

626 3M Company. (2000). *Phase-out Plan for POSF-Based Products*. St. Paul, MN.

627 Abdelaal, F. B., Rowe, R. K., and Islam, M. Z. (2014). “Effect of leachate composition on the
628 long-term performance of a HDPE geomembrane *.” *Geotextiles and Geomembranes*,
629 42(4), 348–362.

630 Aminabhavi, T. M., and Naik, H. G. (1998). “Chemical compatibility testing of geomembranes –
631 sorption/desorption, diffusion, permeation and swelling phenomena.” *Geotextiles and*
632 *Geomembranes*, 16(6), 333–354.

633 Arp, H. P. H., Niederer, C., and Goss, K.-U. (2006). “Predicting the Partitioning Behavior of
634 Various Highly Fluorinated Compounds †.” *Environmental Science & Technology*, 40(23),
635 7298–7304.

636 August, H., and Tatzky, R. (1984). “Permeabilities of Commercially Available Polymeric Liners
637 for Hazardous Landfill Leachate Organic Constituents.” *International Conference on*
638 *Geomembranes*, Denver, CO, 163–168.

639 Barone, F. S., Rowe, R. K., and Quigley, R. M. (1990). “Laboratory determination of chloride

640 diffusion coefficient in an intact shale.” *Canadian Geotechnical Journal*, NRC Research
641 Press Ottawa, Canada , 27(2), 177–184.

642 Barone, F. S., Rowe, R. K., and Quigley, R. M. (1992a). “Estimation of Chloride Diffusion
643 Coefficient and Tortuosity Factor for Mudstone.” *Journal of Geotechnical Engineering*,
644 American Society of Civil Engineers, 118(7), 1031–1045.

645 Barone, F. S., Rowe, R. K., and Quigley, R. M. (1992b). “A laboratory estimation of diffusion
646 and adsorption coefficients for several volatile organics in a natural clayey soil.” *Journal of*
647 *Contaminant Hydrology*, Elsevier, 10(3), 225–250.

648 Benskin, J. P., Li, B., Ikonou, M. G., Grace, J. R., and Li, L. Y. (2012). “Per-and
649 Polyfluoroalkyl Substances in Landfill Leachate: Patterns, Time Trends, and Sources.”
650 *Environmental Science & Technology*, 46, 11532–11540.

651 Bonaparte, R., Daniel, D., and Koerner, R. M. (2002). *Assessment and recommendations for*
652 *improving the performance of waste containment systems*.

653 Buck, R. C., Franklin, J., Berger, U., Conder, J. M., Cousins, I. T., Voogt, P. De, Jensen, A. A.,
654 Kannan, K., Mabury, S. A., and van Leeuwen, S. P. J. (2011). “Perfluoroalkyl and
655 polyfluoroalkyl substances in the environment: Terminology, classification, and origins.”
656 *Integrated Environmental Assessment and Management*, 7(4), 513–541.

657 Busch, J., Ahrens, L., Sturm, R., and Ebinghaus, R. (2010). “Polyfluoroalkyl compounds in
658 landfill leachates.” *Environmental Pollution*, 158, 1467–1471.

659 Crank, J. (1979). *The Mathematics of Diffusion*. Oxford University Press.

660 Deng, S., Zhang, Q., Nie, Y., Wei, H., Wang, B., Huang, J., Yu, G., and Xing, B. (2012).
661 “Sorption mechanisms of perfluorinated compounds on carbon nanotubes.” *Environmental*
662 *Pollution*, 168, 138–144.

663 DiBattista, V., and Rowe, R. K. (2020). “Contaminant Diffusion Through a Novel Coextruded
664 Vapour Barrier.” *Journal of Geotechnical and Geoenvironmental Engineering (in press)*.

665 Eggen, T., Moeder, M., and Arukwe, A. (2010). “Municipal landfill leachates: A significant
666 source for new and emerging pollutants.” *Science of the Total Environment*, 408, 5147–
667 5157.

668 Eun, J., Tinjum, J. M., Benson, C. H., and Edil, T. B. (2017). “Comparison of Volatile Organic
669 Compound Transport in Composite Liners with HDPE and Ethylene-Vinyl Alcohol Co-
670 Extruded Geomembranes.” *Journal of Geotechnical and Geoenvironmental Engineering*,
671 143(6), 1–11.

672 Fuertes, I., Gómez-Lavín, S., Elizalde, M. P., and Urriaga, A. (2017). “Perfluorinated alkyl
673 substances (PFASs) in northern Spain municipal solid waste landfill leachates.”
674 *Chemosphere*, 168, 399–407.

675 Gallen, C., Drage, D., Eaglesham, G., Grant, S., Bowman, M., and Mueller, J. F. (2017).
676 “Australia-wide assessment of perfluoroalkyl substances (PFASs) in landfill leachates.”
677 *Journal of Hazardous Materials*, 331, 132–141.

678 Government of Canada. (2012). *Proposed Risk Management Approach for Perfluorooctanoic
679 Acid (PFOA), its Salts, and its Precursors and Long-Chain (C9-C20) Perfluorocarboxylic
680 Acids (PFCAs), their Salts, and their Precursors*.

681 Hale, S. E., Arp, H. P. H., Slinde, G. A., Wade, E. J., Bjørseth, K., Breedveld, G. D., Straith, B.
682 F., Moe, K. G., Jartun, M., and Høisæter, Å. (2017). “Sorbent amendment as a remediation
683 strategy to reduce PFAS mobility and leaching in a contaminated sandy soil from a
684 Norwegian firefighting training facility.” *Chemosphere*, Elsevier Ltd, 171, 9–18.

685 Health Canada. (2018a). *Guidelines for Canadian Drinking Water Quality: Guideline Technical*

686 Document — *Perfluorooctane Sulfonate (PFOS)*. Ottawa, Ontario.

687 Health Canada. (2018b). *Guidelines for Canadian Drinking Water Quality Guideline Technical*

688 *Document Perfluorooctanoic Acid (PFOA)*. Ottawa, ON.

689 Islam, M. Z., and Rowe, R. K. (2009). “Permeation of BTEX through Unaged and Aged HDPE

690 Geomembranes.” *Journal of Geotechnical and Geoenvironmental Engineering*, 1130–1140.

691 Johnson, R. L., Anschutz, A. J., Smolen, J. M., Simcik, M. F., and Penn, R. L. (2007). “The

692 Adsorption of Perfluorooctane Sulfonate onto Sand, Clay, and Iron Oxide Surfaces.”

693 *Journal of Chemical Engineering Data*, 52(4), 1165–1170.

694 Jones, D. (2016). “Containment of Organic Contaminants using Geosynthetics.” Queen’s

695 University.

696 Jones, D. D., and Rowe, R. K. (2016). “BTEX Migration through Various Geomembranes and

697 Vapor Barriers.” *Journal of Geotechnical and Geoenvironmental Engineering*, 142(10), 1–

698 12.

699 Lagaron, J. M., Powell, A. K., and Bonner, G. (2001). “Permeation of water, methanol, fuel and

700 alcohol-containing fuels in high-barrier ethylene-vinyl alcohol copolymer.” *Polymer*

701 *Testing*, 20, 569–577.

702 Lake, C. B., and Rowe, R. K. (2004). “Volatile organic compound diffusion and sorption

703 coefficients for a needle-punched GCL.” *Geosynthetics International*, 11(4), 257–272.

704 Martin, J. W., Asher, B. J., Beesoon, S., Benskin, J. P., and Ross, M. S. (2010). “PFOS or

705 PreFOS? Are perfluorooctane sulfonate precursors (PreFOS) important determinants of

706 human and environmental perfluorooctane sulfonate (PFOS) exposure?” *Journal of*

707 *Environmental Monitoring*.

708 McWatters, R. S. (2010). “Diffusive Transport of Volatile Organic Compounds through

709 Geomembranes.” Queen’s University.

710 McWatters, R. S., and Rowe, R. K. (2009). “Transport of volatile organic compounds through
711 PVC and LLDPE geomembranes from both aqueous and vapour phases.” *Geosynthetics
712 International*, 16(6), 468–481.

713 McWatters, R. S., and Rowe, R. K. (2010). “Diffusive Transport of VOCs through LLDPE and
714 Two Coextruded Geomembranes.” *Journal of Geotechnical and Geoenvironmental
715 Engineering*, 136(September), 1167–1177.

716 McWatters, R. S., and Rowe, R. K. (2014). “Permeation of Volatile Organic Compounds through
717 EVOH Thin Film Membranes and Coextruded LLDPE / EVOH / LLDPE Geomembranes.”
718 *Journal of Geotechnical and Geoenvironmental Engineering*, 1–14.

719 McWatters, R. S., and Rowe, R. K. (2018). “Barrier permeation properties of EVOH thin-film
720 membranes under aqueous and non-aqueous conditions.” *Geotextiles and Geomembranes*,
721 Elsevier, 46(4), 529–541.

722 McWatters, R. S., Rowe, R. K., Wilkins, D., Spedding, T., Hince, G., Richardson, J., and Snape,
723 I. (2019). “Modelling of vapour intrusion into a building impacted by a fuel spill in
724 Antarctica.” *Journal of Environmental Management*, Elsevier, 231, 467–482.

725 McWatters, R. S., Rowe, R. K., Wilkins, D., Spedding, T., Jones, D., Wise, L., Mets, J., Terry,
726 D., Hince, G., Gates, W. P., Di Battista, V., Shoaib, M., Bouazza, A., and Snape, I. (2016).
727 “Geosynthetics in Antarctica: Performance of a composite barrier system to contain
728 hydrocarbon-contaminated soil after three years in the field.” *Geotextiles and
729 Geomembranes*, 44(2016), 673–685.

730 Milley, S. A., Koch, I., Fortin, P., Archer, J., Reynolds, D., and Weber, K. P. (2018). “Estimating
731 the number of airports potentially contaminated with perfluoroalkyl and polyfluoroalkyl

732 substances from aqueous film forming foam: A Canadian example.” *Journal of*
733 *Environmental Management*, Academic Press, 222, 122–131.

734 Montgomery, J. H., and Welkom, L. M. (1989). *Groundwater Chemicals Desk Reference*. Lewis
735 Publishers Inc., Chelsea, MI.

736 National Institute of Health Sciences. (2020). “Pefluoroalkyl and Polyfluoroalkyl Substances
737 (PFAS).” <<https://www.niehs.nih.gov/health/topics/agents/pfc/index.cfm>> (Mar. 24, 2020).

738 Park, J. K., Hoopes, J. A., and Sakti, J. P. (1995). “Effectiveness of geomembranes as barriers for
739 organic compounds.” Industrial Fabrics Association International, St. Paul, MN (United
740 States).

741 Park, J. K., and Nibras, M. (1993). “Mass flux of organic chemicals through polyethylene
742 geomembranes.” *Water environment research*, Water Environment Federation, 65(3), 227–
743 237.

744 Rayne, S., and Forest, K. (2009). “A comparative assessment of octanol-water partitioning and
745 distribution constant estimation methods for perfluoroalkyl carboxylates and sulfonates.”
746 *Nature Precedings*, Springer Science and Business Media LLC.

747 Rowe, R. K. (1998). “Geosynthetics and the minimization of contaminant migration through
748 barrier systems beneath solid waste.” *Sixth International Conference on Geosynthetics*,
749 Atlanta, GA, 76.

750 Rowe, R. K. (2015). “Reflections on the evolution of geoenvironmental engineering.”
751 *Environmental Geotechnics*, ICE Publishing, 2(2), 65–67.

752 Rowe, R. K., and Badv, K. (1996). “Advective-diffusive contaminant migration in unsaturated
753 sand and gravel.” *Journal of Geotechnical Engineering*, American Society of Civil
754 Engineers (ASCE), 122(12), 965–975.

755 Rowe, R. K., and Booker, J. R. (1985). “Two-dimensional pollutant migration in soils of finite
756 depth.” *Canadian Geotechnical Journal*, NRC Research Press Ottawa, Canada , 22(4),
757 429–436.

758 Rowe, R. K., and Booker, J. R. (2004). “POLLUTE V.7 - 1D Pollutant Migration through a Non-
759 homogenous Soil.” GAEA Environmental Engineering Ltd.

760 Rowe, R. K., Booker, J. R., and Fraser, J. (1997). “POLLUTE v. 6.3: 1D pollutant migration
761 through a non-homogeneous soil.” Distributed by GAEA Environmental Ltd. Whitby,
762 Ontario.

763 Rowe, R. K., Caers, C. J., and Barone, F. (1988). “Laboratory determination of diffusion and
764 distribution coefficients of contaminants using undisturbed clayey soil.” *Canadian*
765 *Geotechnical Journal*, 25(1), 108–118.

766 Rowe, R. K., Jones, D. D., and Rutter, A. (2016a). “Polychlorinated biphenyl diffusion through
767 HDPE geomembrane.” *Geosynthetics International*, 23(6), 408–421.

768 Rowe, R. K., Mukunoki, T., Bathurst, R. J., Rimal, S., Hurst, P., and Hansen, S. (2005). “The
769 Performance of a Composite Liner for Retaining Hydrocarbons under Extreme
770 Environmental Conditions.” *Slopes and Retaining Structures Under Seismic and Static*
771 *Conditions*, American Society of Civil Engineers, Reston, VA, 1–17.

772 Rowe, R. K., Quigley, R. M., Brachman, R. W. I., and Booker, J. R. (2004). *Barrier Systems for*
773 *Waste Disposal Facilities*. E & FN Spon, New York, NY.

774 Rowe, R. K., Saheli, P. T., and Rutter, A. (2016b). “Partitioning and diffusion of PBDEs through
775 an HDPE geomembrane.” *Waste Management*, 55, 191–203.

776 Saheli, P. T., Rowe, R. K., and Rutter, A. (2016). “Diffusion of bisphenol-A (BPA) through an
777 HDPE geomembrane.” *Geosynthetics International*, 23(6), 452–462.

778 Sangam, H. P., and Rowe, R. K. (2001). "Migration of dilute aqueous organic pollutants through
779 HDPE geomembranes." *Geotextiles and Geomembranes*, 19(6), 329–357.

780 US EPA. (2012). "Estimation Programs Interface Suite(TM) for Microsoft Windows, v4.11."
781 United States Environmental Protection Agency, Washington, DC.

782 Yan, H., Cousins, I. T., Zhang, C., and Zhou, Q. (2015). "Perfluoroalkyl acids in municipal
783 landfill leachates from China: Occurrence, fate during leachate treatment and potential
784 impact on groundwater." *Science of The Total Environment*, 524–525, 23–31.

785 Yu, Q., Zhang, R., Deng, S., Huang, J., and Yu, G. (2008). "Sorption of perfluorooctane
786 sulfonate and perfluorooctanoate on activated carbons and resin: Kinetic and isotherm
787 study." *Water Research*, 43, 1150–1158.

788

789

790 **List of Notation**

c	mgL^{-1}	Concentration
D_g	m^2s^{-1}	Diffusion Coefficient
f	$\text{mgm}^{-2}\text{s}^{-1}$	Diffusive flux
H	M	Membrane thickness
$\log K_{ow}$	(-)	<i>n</i> -octanol/water partition coefficient
M	g	Mass
M_w	gmol^{-1}	Molar Mass
P_g	m^2s^{-1}	Permeability Coefficient
pK_a	(-)	Acid dissociation constant
S_{gf}	(-)	Partitioning Coefficient
V	L^3	Volume
Z	Length	Distance
r_g	gcm^{-3}	Geomembrane Density

791

792 **List of Abbreviations**

AFFF	Aqueous film forming foam
BPA	Bisphenol-A
BTEX	Benzene, toluene, ethylbenzene, xylenes
CMC	Critical micelle concentration
CoEx	Coextruded geomembrane (polyethylene/tie layer/EVOH/tie layer/polyethylene)
COV	Coefficient of Variation
DDI	Double De-Ionized
EVOH	Ethylene vinyl alcohol
HDPE	High density polyethylene
LLDPE	Linear low density polyethylene
MSW	Municipal Solid Waste
PBDE	Polybrominated diphenyl ethers
PCB	Polychlorinated biphenyl
PFAS	Per- and polyfluoroalkyl substances

PFOA	Perfluorooctanoate
PFOS	Perfluorooctane sulfonate
TCE	Trichloroethylene

793

Supplemental Materials

Table S1: Analyzed PFOA and PFOS concentrations for all experiments at the most recent sampling events

Material	Temp. (°C)	c_o^a (mg/L)	c_s (mg/L)	c_r (mg/L)	Time (days)
0.1 mm LLDPE	23	19.8 (PFOA)	29 (PFOA)	0.3×10^{-4} (PFOA)	483
		22.7 (PFOS)	23 (PFOS)	0.5×10^{-4} (PFOS)	
0.1 mm CoEx	23	19.8 (PFOA)	14 (PFOA)	BDL (PFOA)	509
		22.7 (PFOS)	17 (PFOS)	3.7×10^{-3} (PFOS)	
0.75 mm LLDPE	23	19.8 (PFOA)	20 (PFOA)	BDL (PFOA)	509
		22.7 (PFOS)	24 (PFOS)	BDL (PFOS)	
0.75 mm CoEx	23	19.8 (PFOA)	26 (PFOA)	0.3×10^{-3} (PFOA)	483
		22.7 (PFOS)	36 (PFOS)	BDL (PFOS)	
0.75 mm CoEx	35	19.8 (PFOA)	34 (PFOA)	0.1×10^{-3} (PFOA)	399
		22.7 (PFOS)	27 (PFOS)	BQL (PFOS)	
0.75 mm CoEx	50	19.8 (PFOA)	24 (PFOA)	0.2×10^{-3} (PFOA)	399
		22.7 (PFOS)	29 (PFOS)	BDL (PFOS)	
0.75 mm LLDPE	35	19.8 (PFOA)	27 (PFOA)	0.2×10^{-3} (PFOA)	399
		22.7 (PFOS)	34 (PFOS)	BDL (PFOS)	
0.75 mm LLDPE	50	19.8 (PFOA)	25 (PFOA)	0.2×10^{-3} (PFOA)	399
		22.7 (PFOS)	29 (PFOS)	BQL (PFOS)	
0.1 mm LLDPE	23	1.1	1.0 (PFOA)	BDL (PFOA)	202
			0.9 (PFOS)	BDL (PFOS)	
0.1 mm LLDPE	35	1.1	1.4 (PFOA)	0.5×10^{-3} (PFOA)	202
			1.0 (PFOS)	BDL (PFOS)	
0.1 mm LLDPE	50	1.1	1.0 (PFOA)	BDL (PFOA)	202
			0.9 (PFOS)	BDL (PFOS)	

^a Individual Concentrations of PFOA and PFOS, unless otherwise stated. Detection limit in receptor = 10^{-4} mg/L

Table S2: Chemical properties and diffusion properties for polyethylene for various compounds

Contaminant	$\log K_{ow}$	M_w	Solubility in water (20°C)	Topological Polar Surface Area ^a	D_g	S_{gf}	P_g
	(-)	(g/mol)	(mg/L)	(Å ²)	(m ² /s)	(-)	(m ² /s)
PFOA – CoEx 0.1 mm	4.81 ^h	414.07	2290-4340 ^b	37.3	-	-	<2.6x10 ⁻¹⁷
PFOS – CoEx 0.1 mm	4.49 ^h	500.13	519-680 ^c	62.8	-	-	<5.5x10 ⁻¹⁷
PFOA – LLDPE 0.1 mm	4.81 ^h	414.07	2290-4340 ^b	37.3	<2.5x10 ⁻¹⁷	0.9-1.4	<3.1x10 ⁻¹⁷
PFOS – LLDPE 0.1 mm	4.49 ^h	500.13	519-680 ^c	62.8	<4x10 ⁻¹⁷	2.8-5.3	<1.6x10 ⁻¹⁶
Benzene ^d	2.15 ⁱ	78.11	1800 ^f	0	2.2x10 ⁻¹³	200	4.4x10 ⁻¹¹
Toluene ^d	2.73 ⁱ	92.14	515 ^f	0	2.2x10 ⁻¹³	350	7.7x10 ⁻¹¹
Ethylbenzene ^d	3.15 ⁱ	106.17	206 ^f	0	1.0x10 ⁻¹³	925	9.2x10 ⁻¹¹
<i>m&p</i> -Xylene ^d	3.15-3.2 ⁱ	106.16	170-200 ^f	0	0.8x10 ⁻¹³	900	7.2x10 ⁻¹¹
<i>o</i> -xylene ^d	3.16 ⁱ	106.16	213 ^f	0	0.8x10 ⁻¹³	900	7.2x10 ⁻¹¹
PCBs Aroclor 1242 ^e	6.98 ^h	291.98	0.24 ^e	0	5-50x10 ⁻¹⁵	90,000-325,000	0.45-16x10 ⁻⁹
BPA ^f	3.64 ^f	228.29	120-380 ^f	40.5	-	-	2.9x10 ⁻¹⁵
Phenol ^f	1.46 ^f	94.11	90,000 ^f	20.2	1.7x10 ⁻¹⁴	3.48	5.9x10 ⁻¹⁴
PBDE (DE-71 Mixture) ^g	6.81-7.90 ^g	564.7	0.0133 ^g	9.2	4x10 ⁻¹⁵	1,800,000	7.2x10 ⁻⁹

^aCalculated using Cactvs 3.4.6.11 (National Center for Biotechnology Information. PubChem Database 2019)

^b(National Center for Biotechnology Information. PubChem Database 2020a)

^c(National Center for Biotechnology Information. PubChem Database 2020b)

^dLLDPE (DiBattista and Rowe 2019)

^eHDPE (Rowe et al. 2016a)

^fHDPE (Saheli et al. 2016)

^gHDPE (Rowe et al. 2016b)

^hCalculated using US EPA Industry Interface Estimation Suite (US EPA 2012)

ⁱ(Montgomery and Welkom 1989)

Table S3: Predicted Source and Receptor Concentrations at 483 days using Sangam and Rowe (2001) Correlations ($P_g=D_g$, $S_{gf}=1$); $c_o=19.8$ mg/L (PFOA) $c_o=22.7$ mg/L (PFOS) for 0.1 mm LLDPE.

	c_{s483d} (mg/L)	c_{r483d} (mg/L)
[R2] $P_{gPFOA}=2.0 \times 10^{-12}$ m ² /s	14.2 (PFOA) ^a	
$P_{gPFOS}=5.5 \times 10^{-13}$ m ² /s	16.3 (PFOS) ^a	
[R3] $P_{gPFOA}=6.6 \times 10^{-106}$ m ² /s	19.8 (PFOA)	<10 ⁻⁴⁸ (PFOA)
$P_{gPFOS}=9.4 \times 10^{-170}$ m ² /s	22.7 (PFOS)	<10 ⁻⁴⁸ (PFOS)
[R4] $D_{gPFOA}=1.4 \times 10^{-16}$ m ² /s	19.76 (PFOA)	0.087 (PFOA)
$D_{gPFOS}=7.4 \times 10^{-17}$ m ² /s	22.64 (PFOS)	0.138 (PFOS)

^aEquilibrium reached

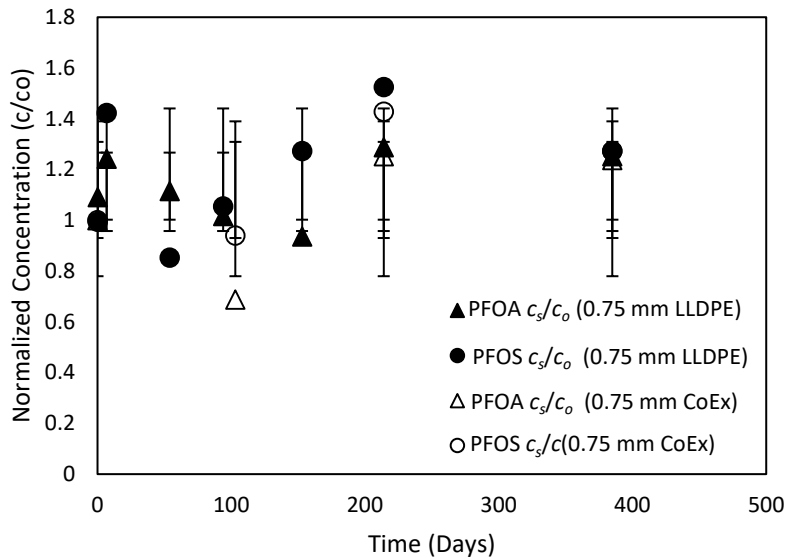


Figure 3: Normalized source concentrations for 0.75 mm LLDPE and 0.75 mm CoEx at 50°C; $c_o=19.8$ ppm (PFOA) and $c_o=22.7$ ppm (PFOS)

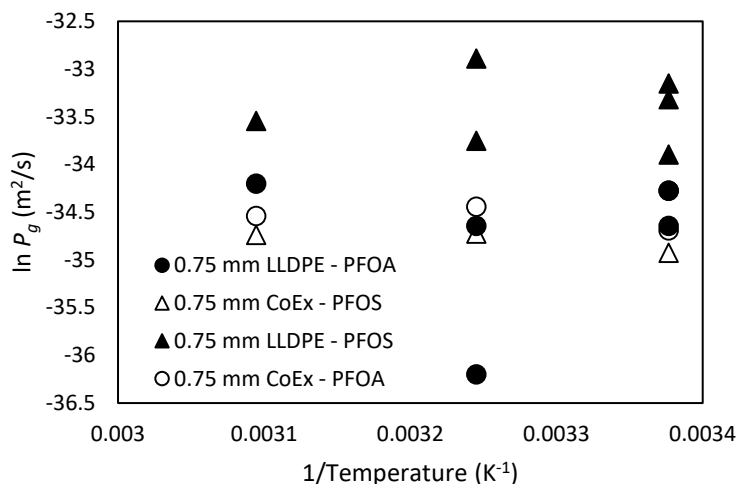


Figure S2: Arrhenius plot for 0.75 mm LLDPE and CoEx at 23°C, 35°C, and 50°C

References

- Jones, D. (2016). "Containment of Organic Contaminants using Geosynthetics." Queen's University.
- Montgomery, J. H., and Welkom, L. M. (1989). *Groundwater Chemicals Desk Reference*. Lewis Publishers Inc., Chelsea, MI.
- National Center for Biotechnology Information. PubChem Database. (2019). "Cactvs 3.4.6.11."
- National Center for Biotechnology Information. PubChem Database. (2020a). "Perfluorooctanoic acid, CID=9554." <<https://pubchem.ncbi.nlm.nih.gov/compound/Perfluorooctanoic-acid>> (Jun. 28, 2020).
- National Center for Biotechnology Information. PubChem Database. (2020b). "Perfluorooctanesulfonic acid, CID=74483." <<https://pubchem.ncbi.nlm.nih.gov/compound/Perfluorooctanesulfonic-acid>> (accessed on June 28, 2020) (Jun. 28, 2020).
- Rowe, R. K., Jones, D. D., and Rutter, A. (2016a). "Polychlorinated biphenyl diffusion through HDPE geomembrane." *Geosynthetics International*, 23(6), 408–421.
- Rowe, R. K., Saheli, P. T., and Rutter, A. (2016b). "Partitioning and diffusion of PBDEs through an HDPE geomembrane." *Waste Management*, 55, 191–203.
- Saheli, P. T., Rowe, R. K., and Rutter, A. (2016). "Diffusion of bisphenol-A (BPA) through an HDPE geomembrane." *Geosynthetics International*, 23(6), 452–462.